ChemComm

COMMUNICATION

View Article Online
View Journal | View Issue

Cite this: *Chem. Commun.*, 2021, 57, 6392

Received 10th April 2021,
Accepted 18th May 2021

DOI: 10.1039/d1cc01907d

rsc.li/chemcomm

Monitoring excited-state relaxation in a molecular marker in live cells–a case study on astaxanthin†

Tingxiang Yang, [ab] Avinash Chettri, [ab] Basseem Radwan, [cd] Ewelina Matuszyk, [c] Malgorzata Baranska [cd] and Benjamin Dietzek *[ab]

Small molecules are frequently used as dyes, labels and markers to visualize and probe biophysical processes within cells. However, very little is generally known about the light-driven excited-state reactivity of such systems when placed in cells. Here an experimental approach to study ps time-resolved excited state dynamics of a benchmark molecular marker, astaxanthin, in live human cells is introduced.

Astaxanthin (AXT, 3,30-dihydroxy-β,β-carotene-4,40-dione), a xanthophyll carotenoid pigment, is found in aquatic animals, *e.g.* salmonids and shrimp.[1,2] The optical properties and excited-state relaxation pathways of this natural pigment have been studied intensively.[3,4] Upon optical excitation into the S_2 state, the molecule undergoes fast internal conversion to the S_1 state.[5,6] In contrast to many keto-carotenoids, the S_1 lifetime of AXT is solvent polarity-independent (*ca.* 5 ps).[7,8] As the chromophore in the carotenoprotein α-crustacyanin AXT has a drastically shorter excited state lifetime (1.8 ps).[7] Upon aggregation of AXT, the lifetime of the AXT excited-state gets prolonged and spectral characteristics of aggregate formation become apparent.[9–12] Formation of H1 and H2-aggregates yields S_1 lifetimes of 17 and 30 ps, respectively, while the S_1 lifetime is 14 ps in J-aggregates.[11] Aside from comprehensive photophysical studies, AXT has drawn attention in biomedical and biophysical research due to its anti-oxidative activity,[13] which is about 10 times higher than those of *e.g.* lutein, zeaxanthin and β-carotene.[14] Consequently, AXT has been evaluated to inhibit the growth of tumour cells.[15,16] In biophysical research AXT has been introduced as a marker for cellular imaging.[17,18] AXT stains lipids in cells,[19] rendering lipid-containing structures easily detectable by resonance Raman microscopy. Thereby, the distribution of lipids, changes in the lipid composition and lipid-associated disease mechanisms have been elucidated.[20,21] Some of us recently employed AXT as a marker to study endothelial cells by resonance Raman spectroscopy.[20] We could show that the prominent C=C stretching band shifts to about 1522 cm^{-1} in the nuclear membrane and to 1524 cm^{-1} in lipid droplets,[17,20] compared to the band position in dimethyl sulfoxide (DMSO, 1520 cm^{-1}),[22] in acetone (1523 cm^{-1}),[23] and in 10% acetone–water solutions where AXT forms aggregates (1518 cm^{-1}).[24] The band shift indicates that conformational changes of AXT might happen in the cellular organelles as compared to isolated AXT in solution. However, the position of the Raman active vibrational band reports on ground-state properties of the molecule. In order to add information on the excited state dynamics upon incorporation of AXT as a marker into human cells, we perform transient absorption studies on living MCF-7 cells.

To identify suitable probe-wavelengths for the *in cellulo* pump–probe studies of the excited-state dynamics of AXT, transient absorption (TA) spectra of AXT in DMSO upon excitation of the S_2 state at 510 nm are shown in Fig. 1. A ground state bleach coincides with the inverted steady-state absorption spectrum of AXT. It is accompanied by strong excited-state absorption (ESA) between 545 and 780 nm. We choose the probe-wavelength at 625 nm to coincide with the maximum of the ESA band in the *in cellulo* experiments (*vide infra*). The reference data of AXT in DMSO reveal an overall decay of the signal with a 5.3 ps time constant, in line with the literature reporting the S_1 lifetime of AXT to vary from 4.3 to 5.6 ps depending on the solvent.[7,25]

To investigate the impact of the cellular environment on the dynamics of the S_1 state in AXT, when taken up by human cells, we utilized a recently reported setup,[26] which allows for studying pump–probe data from adherently growing cells. The setup (see Fig. 2a) has been introduced to study fixed cells;[26]

[a] *Leibniz Institute of Photonic Technology (Leibniz-IPHT), Albert-Einstein-Strabe 9, Jena 07745, Germany. E-mail: benjamin.dietzek@leibniz-ipht.de*
[b] *Institute of Physical Chemistry and Abbe Center of Photonics, Friedrich Schiller University Jena, Helmholtzweg 4, Jena 07743, Germany*
[c] *Jagiellonian Centre for Experimental Therapeutics (JCET), Jagiellonian University, 14 Bobrzynskiego Str., Krakow 30-348, Poland*
[d] *Faculty of Chemistry, Jagiellonian University, 2 Gronostajowa Str., Krakow 30-387, Poland*

† Electronic supplementary information (ESI) available. See DOI: 10.1039/d1cc01907d

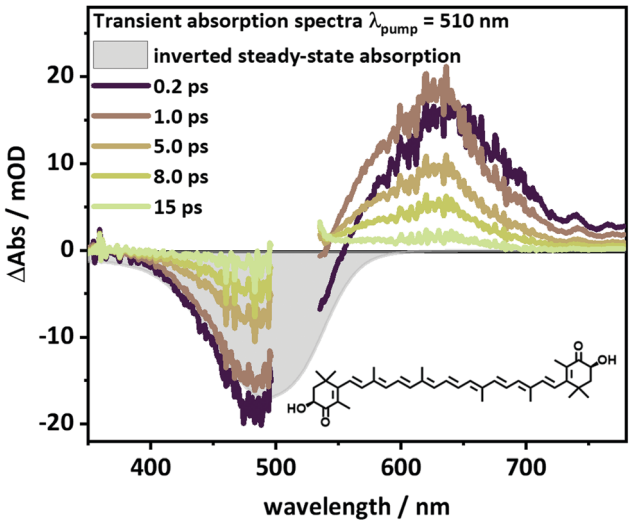

Fig. 1 Transient absorption spectra of AXT with λ_{pump} = 510 nm at selected delay times, with filled and scale-inverted steady-state absorption spectrum as reference for ground-state bleaching (GSB) and the molecular structure of AXT. Data were collected in DMSO in a 1 mm cuvette.

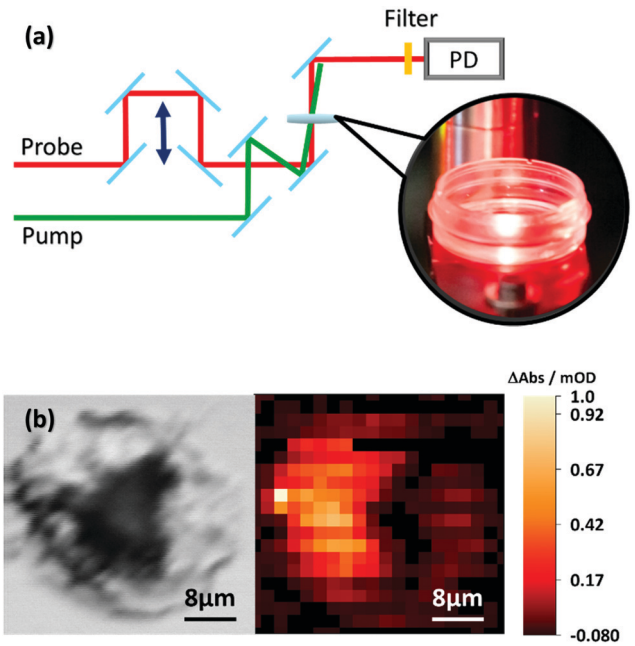

Fig. 2 (a) Schematic of the time-resolved pump probe setup. Pump and probe beams are overlapped in space and time. After interacting with the sample, the probe beam is sent to PD, the photodiode. (b) Phase image (left panel) focused inside of the MCF7 cell and the distribution of AXT (right panel) in the cell obtained by transient absorption microscopy (λ_{pump} = 470 nm, and λ_{probe} = 625 nm).

however, live cell studies have not yet been performed. The sample is placed in a μ-dish, while in principle an incubator can be inserted at the sample position. The pump and probe pulses are weakly focussed so that the area of the cell sample illuminated during one experimental run is 200–300 μm, *i.e.* the signal is averaged over several MCF-7 cells (cell size of *ca.* 30 μm). Thus, the *in cellulo* transient absorption setup complements the experimentally more demanding transient absorption microscopy,[27] which has been utilized before, *e.g.* to localize nanoparticles in live cells.[28–30] Still the experiments are capable of addressing possible alterations in the AXT excited state relaxation upon uptake into cells.

For the *in cellulo* experiments MCF-7 cells are dosed with 10 μM of AXT for 24 hours. Under these conditions the cell viability is about 93% (see Fig. S3, ESI†). After 24 hours of incubation in RPMI 1640 medium (Sigma-Aldrich), the medium is removed and the cells are washed three times with phosphate-buffered saline (PBS) (Sigma-Aldrich). The cells are divided into two sub-sets. One set of cells is fixed with 4% phosphate-buffered formaldehyde (Carl Roth, Germany) and stored at 37 °C with a humidified atmosphere containing 5% CO_2 for 15 min before the μ-dishes are rinsed twice with PBS. The second set of cells is directly suspended in 1 mL PBS before being transferred immediately to the *in cellulo* transient absorption experiment. We record the images of both fixed (see Fig. 3a) and live cells (see Fig. 3b) stained with trypan blue. The stain confirms that after incubating with AXT the cells are indeed still alive. The actual uptake of AXT into the MCF-7 cells is validated by transient absorption microscopy (see Fig. 2b). A phase image (see the left panel of Fig. 2b) shows the fixed cells' structure. The transient absorption microscopy image (see the right panel of Fig. 2b, pump at 470 nm, probe at 625 nm, and pump–probe delay Δt = 3 ps) confirms the presence of AXT inside the cells and shows that the carotenoid is not observed in the nucleus. The high concentrations of AXT in the cytoplasm are in line with previous reports on AXT accumulation in lipid-rich compartments of cells.[20]

During the *in cellulo* transient absorption experiments the sample was excited at 510 nm with an average excitation power of 10 μW. The *in cellulo* transient absorption data show instantaneous appearance of ground state bleach (probed at 465 nm) and excited state absorption (at 625 nm; see Fig. 3e). The ESA at 625 nm decays with a characteristic lifetime of 5.7 and 5.3 ps for live and fixed cells, respectively. We recorded excited state kinetics during two consecutive experimental runs and did not observe photobleaching or differences in the kinetics that might be attributed to prolonged exposure to the pump light (see inset in Fig. 3e). The S_1 lifetimes of AXT in live (5.7 ps) and fixed MCF-7 cells (5.3 ps) agree with the S_1 lifetime of AXT in DMSO solution (5.3 ps) indicating that the transient absorption signal detected stems from isolated carotenoids as opposed to aggregates, which have been shown to have significantly longer-lived S_1 states.[11,31]

Cell viability after the *in cellulo* pump–probe spectroscopy is evaluated by removal of the PBS buffer from the Petri dishes and subsequent staining of the cells with 60 μL of 0.4% trypan blue (dead cell stain, Gibco, USA) in 1 mL of Hanks' balanced salt solution (HBSS) (Sigma-Aldrich). After staining for 2 minutes the cells are rinsed twice with HBSS. The cells are accessed in an inverted Axiovert 25 microscope (Carl Zeiss, Germany). The corresponding images are recorded by a Raspberry Pi camera (see Fig. 3c and d). The data show neither significant

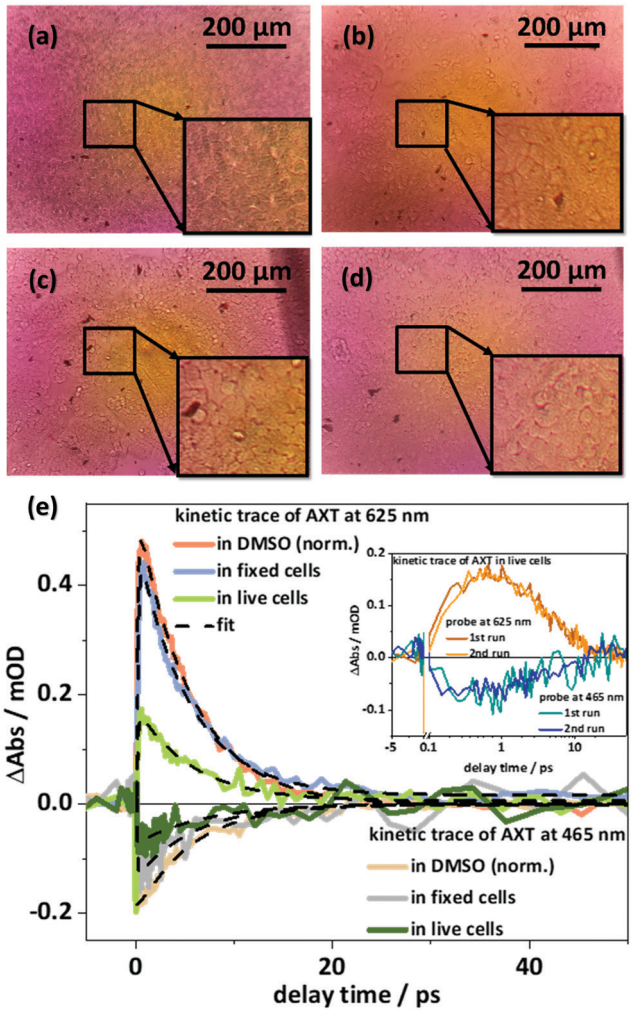

Fig. 3 (a) The fixed cells stained with trypan blue. (b) The live cells stained with trypan blue before laser pulse. (c) The live cells without trypan blue before measuring. (d) The same detected area as (c) after measuring and treating with trypan blue. The black areas on the top right side of (c and d) are the markers of the measured areas for recording the same cells' areas before and after experiments. The yellow areas in the centre of (a–d) are caused by the lamp of the microscope. (e) The kinetic traces of AXT probed at 465 nm and 680 nm measured in live cells and fixed cells, as well as in DMSO solvent. The inset in (e) compares the data of the first and second experimental runs sampling the same area in the bulk of cells (λ_{pump} = 510 nm).

changes in cellular shape nor uptake of trypan blue, which would result in significant coloration of the cells, as *e.g.* seen for the dead cells depicted in Fig. 3a. Thus, our experimental setup allows the excited-state kinetics of AXT to be recorded in live cells.

The photoinduced dynamics in AXT recorded *in cellulo* appears to be unchanged compared to the dynamics recorded in solution. Aside from indicating the absence of AXT aggregation in the cells, this points to the fact that structural distortion of the AXT molecules, which has been suggested based on shifts of the resonance Raman active C=C vibration, do not alter the transient absorption data recorded during the *in cellulo* experiments. Finally, in a methodological context we show that our approach to *in cellulo* transient absorption spectroscopy offers a valuable path to study the impact of local environments on the photoinduced dynamics in stains, markers and beyond this in light-activated drugs, *e.g.* for photodynamic therapy,[32] and interactions between phototherapy agents and live cells.

We thank Prof. Dr Rainer Heintzmann and Dr Benedict Diederich for providing BioLab facilites supporting the image acquisition. The research has been supported by the European Union (*via* the ITN LogicLab funded under the Horizon 2020 research and innovation program under the grant agreement No. 813920) and the German Science Foundation (*via* the grant No. 395358570).

Conflicts of interest

There are no conflicts to declare.

Notes and references

1 W. Miki, K. Yamaguchi and S. Konosu, *Comp. Biochem. Physiol., Part B: Biochem. Mol. Biol.*, 1982, **71**, 7–11.
2 R. T. Lorenz and G. R. Cysewski, *Trends Biotechnol.*, 2000, **18**, 160–167.
3 M. Buchwald and W. P. Jencks, *Biochemistry*, 1968, **7**, 834–843.
4 T. Polivka, C. A. Kerfeld, T. Pascher and V. Sundstrom, *Biochemistry*, 2005, **44**, 3994–4003.
5 H. H. Billsten, J. Pan, S. Sinha, T. Pascher, V. Sundstrom and T. Polivka, *J. Phys. Chem. A*, 2005, **109**, 6852–6859.
6 T. Polívka and V. J. C. R. Sundström, *Chem. Rev.*, 2004, **104**, 2021–2072.
7 R. P. Ilagan, R. L. Christensen, T. W. Chapp, G. N. Gibson, T. Pascher, T. Polivka and H. A. Frank, *J. Phys. Chem. A*, 2005, **109**, 3120–3127.
8 D. Zigmantas, R. G. Hiller, F. P. Sharples, H. A. Frank, V. Sundström and T. Polívka, *Phys. Chem. Chem. Phys.*, 2004, **6**, 3009–3016.
9 R. Giovannetti, L. Alibabaei and F. Pucciarelli, *Spectrochim. Acta, Part A*, 2009, **73**, 157–162.
10 M. Zannotti, R. Giovannetti, B. Minofar, D. Reha, L. Plackova, C. A. D'Amato, E. Rommozzi, H. V. Dudko, N. Kari and M. Minicucci, *Spectrochim. Acta, Part A*, 2018, **193**, 235–248.
11 M. Fuciman, M. Durchan, V. Šlouf, G. Keşan and T. Polívka, *Chem. Phys. Lett.*, 2013, **568–569**, 21–25.
12 A. J. Musser, M. Maiuri, D. Brida, G. Cerullo, R. H. Friend and J. Clark, *J. Am. Chem. Soc.*, 2015, **137**, 5130–5139.
13 M. Guerin, M. E. Huntley and M. Olaizola, *Trends Biotechnol.*, 2003, **21**, 210–216.
14 W. Miki, *Pure Appl. Chem.*, 1991, **63**, 141–146.
15 P. Palozza, C. Torelli, A. Boninsegna, R. Simone, A. Catalano, M. C. Mele and N. Picci, *Cancer Lett.*, 2009, **283**, 108–117.
16 B. McCall, C. K. McPartland, R. Moore, A. Frank-Kamenetskii and B. W. Booth, *Antioxidants*, 2018, **7**(10), 135.
17 A. Kaczor and M. Baranska, *Anal. Chem.*, 2011, **83**, 7763–7770.
18 A. Kaczor, K. Turnau and M. Baranska, *Analyst*, 2011, **136**(6), 1109–1112.
19 K. Li, J. Cheng, Q. Ye, Y. He, J. Zhou and K. Cen, *Bioresour. Technol.*, 2017, **244**, 1439–1444.
20 K. Czamara, A. Adamczyk, M. Stojak, B. Radwan and M. Baranska, *Cell. Mol. Life Sci.*, 2021, **78**, 3477–3484.
21 B. Radwan, A. Adamczyk, S. Tott, K. Czamara, K. Kaminska, E. Matuszyk and M. Baranska, *Molecules*, 2020, **25**, 5752.
22 M. Dudek, G. Zajac, A. Kaczor and M. Baranska, *J. Phys. Chem. B*, 2016, **120**, 7807–7814.
23 R. J. H. Clark, N. R. Durso and P. F. Zagalsky, *J. Am. Chem. Soc.*, 1980, **102**, 6693–6698.
24 V. R. Salares, N. M. Young, P. R. Carey and H. J. Bernstein, *J. Raman Spectrosc.*, 1977, **6**, 282–288.

25 R. M. Han, Y. X. Tian, Y. S. Wu, P. Wang, X. C. Ai, J. P. Zhang and L. H. Skibsted, *Photochem. Photobiol.*, 2006, **82**, 538–546.
26 K. R. A. Schneider, A. Chettri, H. D. Cole, K. Reglinski, J. Bruckmann, J. A. Roque, 3rd, A. Stumper, D. Nauroozi, S. Schmid, C. B. Lagerholm, S. Rau, P. Bauerle, C. Eggeling, C. G. Cameron, S. A. McFarland and B. Dietzek, *Chem. – Eur. J.*, 2020, **26**, 14844–14851.
27 D. y. Davydova, A. de la Cadena, D. Akimov and B. Dietzek, *Laser Photonics Rev.*, 2016, **10**, 62–81.
28 L. Tong, Y. Liu, B. D. Dolash, Y. Jung, M. N. Slipchenko, D. E. Bergstrom and J. X. Cheng, *Nat. Nanotechnol.*, 2011, **7**, 56–61.
29 T. Chen, F. Lu, A. M. Streets, P. Fei, J. Quan and Y. Huang, *Nanoscale*, 2013, **5**, 4701–4705.
30 L. Zhang, S. Shen, Z. Liu and M. Ji, *Adv. Biosyst.*, 2017, **1**, e1700013.
31 H. H. Billsten, V. Sundstrom and T. Polivka, *J. Phys. Chem. A*, 2005, **109**, 1521–1529.
32 S. Monro, K. L. Colón, H. Yin, J. Roque, P. Konda, S. Gujar, R. P. Thummel, L. Lilge, C. G. Cameron and S. A. McFarland, *Chem. Rev.*, 2018, **119**, 797–828.